JOURNAL OF GEOPHYSICAL RESEARCH, VOL. 114, B05306, doi:10.1029/2007JB005518, 2009

Variability of repeating earthquake behavior along the Longitudinal Valley fault zone of eastern Taiwan

Kate Huihsuan Chen,[1] Ruey-Juin Rau,[2] and Jyr-Ching Hu[3]

Received 22 November 2007; revised 12 January 2009; accepted 5 March 2009; published 23 May 2009.

[1] Two major clusters of repeating earthquake sequences (RES) are found on two fault patches near the Longitudinal Valley fault (LVF) in eastern Taiwan, the Chihshang segment to the south and the Hualien segment to the north. The 25 M 2.3–4.6 RES on the Hualien segment are widely distributed in a NNE direction over a distance of 45 km, whereas on the Chihshang segment, the 30 M 2.2–3.4 RES have a shorter along-strike extent of about 15 km. The longer spatial extent of RES on the Hualien segment may indicate a wider distributed creeping zone at depth. $M \geq 3.8$ RES are observed on the Hualien segment and are characterized by quasiperiodic recurrence. Statistical analysis of the size and number of earthquakes adjacent to the RES indicates that the smaller number of large earthquakes in the vicinity may explain the quasiperiodic recurrence of RES. We argue that on the Hualien segment, $M\sim4$ or larger earthquakes are isolated enough in space to facilitate the occurrence of repeated ruptures.

Citation: Chen, K. H., R.-J. Rau, and J.-C. Hu (2009), Variability of repeating earthquake behavior along the Longitudinal Valley fault zone of eastern Taiwan, *J. Geophys. Res.*, *114*, B05306, doi:10.1029/2007JB005518.

1. Introduction

[2] A repeating earthquake sequence consists of a series of repeated events rupturing on the same fault patch. The recurrence of earthquakes is suggestive of a renewal process taking place in the fault zone. The recurrence times are, in general, inversely proportional to the average slip rate on the fault [e.g., *Scholz*, 1990; *Nadeau and Johnson*, 1998; *Schaff et al.*, 1998; *Nadeau and McEvilly*, 1999, 2004; *Beeler et al.*, 2001; *Bürgmann et al.*, 2000]. Why the earthquakes repeat, what controls their regularity in size and time, and how the recurrence parameters reflect variations in fault zone properties are questions of fundamental importance to understanding the earthquake cycle with important implications for regional earthquake probability and risk estimates [*Working Group on California Earthquake Probabilities*, 2003]. Mechanical analog models have suggested that less stress interaction with neighboring faults/asperities may lead to more regular earthquake recurrences and smaller variations in earthquake sizes [e.g., *Ben-Zion and Rice*, 1995; *Lynch et al.*, 2003; *Kato*, 2004; *Zöller et al.*, 2005]. In nature, the factors controlling the recurrence parameters (i.e., regularity in size and time, recurrence interval, and occurrence lifetime) are likely more complicated, and the mechanisms of these processes are not yet understood.

[3] Repeating events have been documented recently near the 160-km-long Longitudinal Valley that represents the plate suture in eastern Taiwan. These events have been inferred to constitute two distinct fault segments separated by ~40 km [*Rau et al.*, 2007; *Chen et al.*, 2008] (Figure 1). Similarities and differences in RES behavior between the two fault segments allow us to study factors controlling the recurrence parameters in a natural fault system. We have previously found that while the Chihshang segment in the south produces only $M < 3.5$ repeating events, the Hualien segment in the north has repeating events with magnitudes larger than 3.8 (M 3.8–4.6 for three RES) in addition to repeating events of magnitude less than 3.8. Notably, the M 3.8–4.6 RES on the Hualien segment are characterized by regular recurrence intervals and small variations in event size. In this study, we aim to answer the following questions: (1) Why are the $M \geq 3.8$, quasiperiodic RES observed on the Hualien segment but not the Chihshang segment? (2) What factors control the similarity and difference in recurrence intervals, regularity in time and size, and occurrence lifetimes of the RES between these two segments?

2. Longitudinal Valley Fault Zone in Eastern Taiwan

[4] As an active plate boundary between the Philippine Sea Plate (PSP) and Eurasian Plate (EP) with a convergence rate of 8 cm/a, the Longitudinal Valley in eastern Taiwan is an example of extreme strain concentration in an oblique collision zone [e.g., *Angelier et al.*, 1997]. The Longitudinal Valley fault (LVF) is an active reverse fault with a left-lateral strike-slip component, especially in the southern part [e.g., *Barrier et al.*, 1982]. The surface deformation pattern is highly variable along the LVF. In the south, where the

[1]Department of Earth Sciences, National Taiwan Normal University, Taipei, Taiwan.
[2]Department of Earth Sciences, National Cheng Kung University, Tainan, Taiwan.
[3]Department of Geosciences, National Taiwan University, Taipei, Taiwan.

0148-0227/09/2007JB005518$09.00

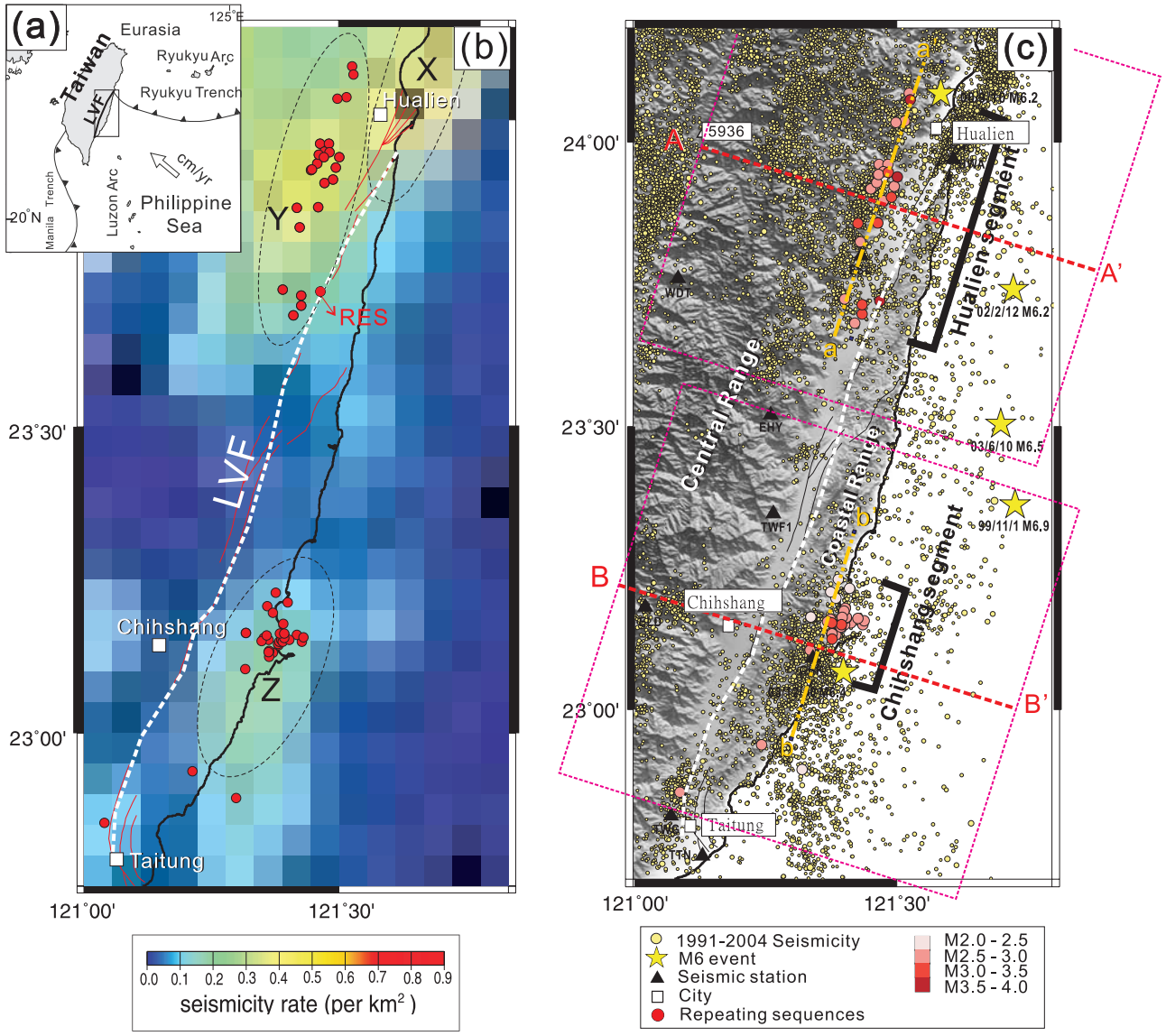

Figure 1. (a) Geodynamic framework of Taiwan. Open arrow indicates relative motion between Philippine Sea plate and Eurasian plate in the Taiwan region. (b) Seismicity rate map of eastern Taiwan using the 1991–2004 earthquake catalogs. Three areas with relatively high earthquake activity are circled using black dashed lines. Red circles indicate location of each RES. (c) Relocated seismicity in eastern Taiwan. $M \geq 2$ earthquakes relocated by HypoDD [*Waldhauser and Ellsworth*, 2000] during the study period are shown in yellow circles. Locations of the RES are shown as red circles with filled colors/shades keyed to their magnitudes. Yellow stars are the $M \geq 6$ earthquakes that occurred in the study region. Seismic stations in eastern Taiwan are denoted by black triangles. Surface trace of the LVF along the boundary between the Longitudinal Valley and Coastal Range is denoted by dashed white line. Active faults along the Longitudinal Valley are shown by solid lines. Dashed lines and boxes indicate cross sections A-A′, B-B′, and the selected earthquakes for Figure 2. Red dashed lines indicate cross sections a-a′ and b-b′ for Figure 12.

most active creep occurs, the deformation is characterized by high-angle reverse faulting at a high slip rate of 3.2 cm/a in a N38°W direction [*Yu and Kuo*, 2001]. In the middle portion of the LVF, the surface slip rate measured by GPS observations is about 2.2 cm/a in a N43°W direction [*Yu and Kuo*, 2001]. In the northern portion, the surface slip rate is 1.1 cm/a in a N10°W direction [*Yu and Kuo*, 2001].

[5] $M \geq 7$ earthquakes in eastern Taiwan occurred in 1908, 1919, 1937, 1938, 1951, 1957, and 1986. Of these major events, the most significant earthquake sequence occurred in 1951. The "1951 Hualien-Taitung earthquake sequence" was composed of twelve $M \geq 6$ events which jointly caused several surface ruptures from the northern to southern LVF [*Gutenberg and Richter*, 1954; *Lee et al.*, 1978; *Abe*, 1981; *Hsu*, 1985; *Cheng et al.*, 1996]. Earthquake relocation and focal mechanism solutions for the past several decades suggest a strong spatial variation along the LVF [*Kuochen et al.*, 2004]. In the southern LVF, there are

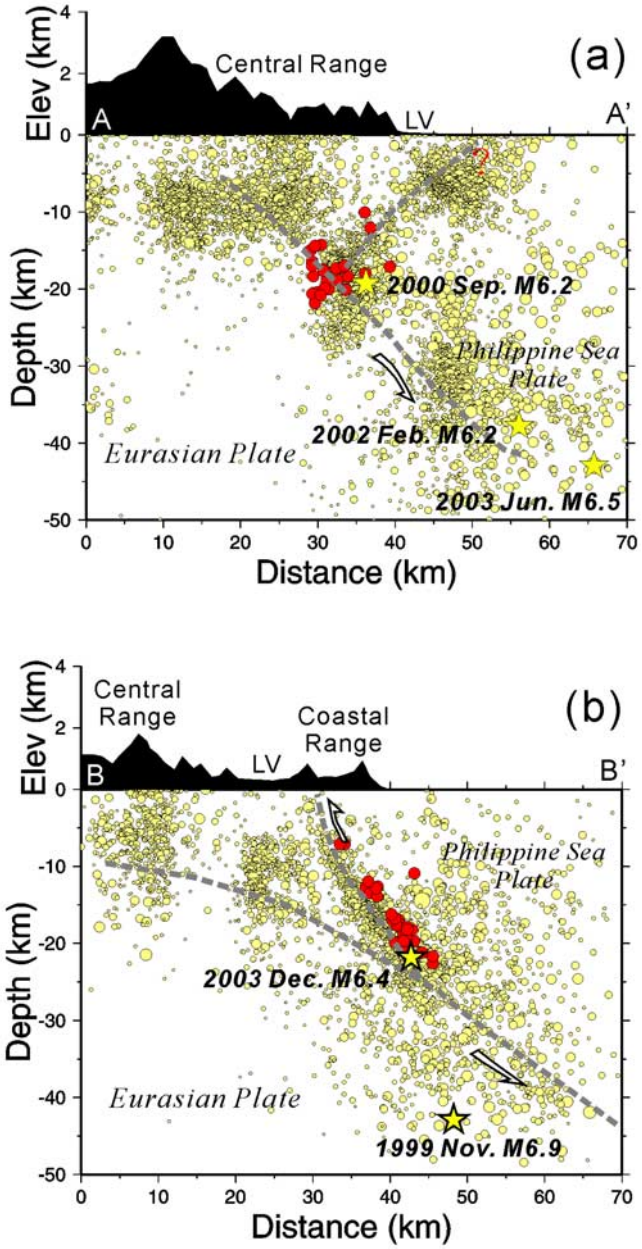

Figure 2. (a) Cross section for the Hualien segment (A-A′). (b) Cross section for the Chihshang segment (B-B′). The 1991–2004 background seismicity and $M \geq 6$ events are denoted by yellow circles and stars, respectively. A schematic crustal model denoted by dashed lines is modified from *Kuochen et al.* [2004].

high rates of microseismicity (Figure 1) with a dominant thrust component and subordinate strike-slip component [*Kao and Jian*, 2001]. In the middle portion, seismicity activity has been sparse during the last two decades (Figure 1), suggesting that this seismic gap is likely to be locked. In the northern LVF, there is a relatively high frequency of large earthquakes with varying types of faulting, indicating a stress regime from compression to transpression [e.g., *Hu et al.*, 1996; *Wu et al.*, 1997; *Kao et al.*, 1998]. *Kuochen et al.* [2004] proposed a boundary at latitude 23.5°N separating the tectonics of eastern Taiwan into two distinct structures. To the south, the EP subducts to the east beneath the PSP, where the fault segment is a suture zone dipping to the east. To the north, the EP dips to the east and the PSP bends and dips to the west, where the fault segment is more complex. The fault model of *Kuochen et al.* [2004] is shown schematically by the dashed line in Figure 2.

[6] Creeping crustal faults often generate microearthquakes, and may also produce large earthquakes that rupture the brittle crust [*Scholz*, 1990]. The LVF in eastern Taiwan has been known to undergo 1–3 cm/a surface creep [e.g., *Yu and Kuo*, 2001] and is probably one of the most active creeping thrust faults known in the world. Because of limited geodetic coverage in this area, however, a well-resolved picture of deep fault behavior is lacking. Interferometric synthetic aperture radar (InSAR) data provide good spatial sampling of the deformation field [e.g., *Massonnet et al.*, 1993], but the nature of land cover and atmospheric conditions in the area complicate the task of obtaining more detailed deformation information [*Hsu and Bürgmann*, 2006]. Studies of repeating earthquakes have been proposed to yield critical parameters associated with a variety of fault zone processes such as fault slip rate variations at depth [e.g., *Bürgmann et al.*, 2000; *Nadeau and McEvilly*, 1999, 2004] and subsurface changes in seismic wave propagation properties [e.g., *Schaff and Beroza*, 2004; *Peng and Ben-Zion*, 2005; *Rubinstein et al.*, 2007]. Observations of repeating earthquakes, if they exist, may provide new insight into the variability of deep fault behavior along the Longitudinal Valley fault zone.

3. Identification of Repeating Earthquakes

[7] Repeating earthquakes are generally identified by high waveform similarity [*Nadeau et al.*, 1995; *Matsuzawa et al.*, 2002; *Igarashi et al.*, 2003; *Uchida et al.*, 2003; *Nadeau and McEvilly*, 2004; *Matsubara et al.*, 2005] and earthquake colocation [e.g., *Vidale et al.*, 1994; *Ellsworth*, 1995; *Rubin et al.*, 1999; *Schaff and Beroza*, 2004]. Establishing an effective colocation of repeating events using relative event relocation methods can be problematic in offshore regions where the spatial coverage of seismic stations is sparse or one sided, where significant changes in station distribution occur over time, or where routine catalog origin times are inaccurate [e.g., *Ross et al.*, 2001]. Inaccurate or inconsistent timing of recorded data can also contribute substantially to inaccurate relative relocations [*Rubin*, 2002] and cause repeating events to be either missed or erroneously included in repeating sequences. Similarly, missed repeats and/or the inclusion of nonrepeating events into sequences can also occur using waveform similarity as a criterion, particularly when the signal-to-noise ratio (SNR) is low, short data windows are employed, and/or when excessive filtering of the waveforms is used [*Uchida et al.*, 2003].

[8] To overcome such problems, we have adopted a more robust approach to identifying RES. This composite selection approach incorporates both waveform similarity (cross-correlation coefficient, ccc) and differential S-P (dS_mP) time information (at subsample precision) and allows exclusion of outliers from the ccc and dS_mP data. By relying only on ccc and dS_mP time statistics for each station considered, the method also effectively eliminates errors introduced by

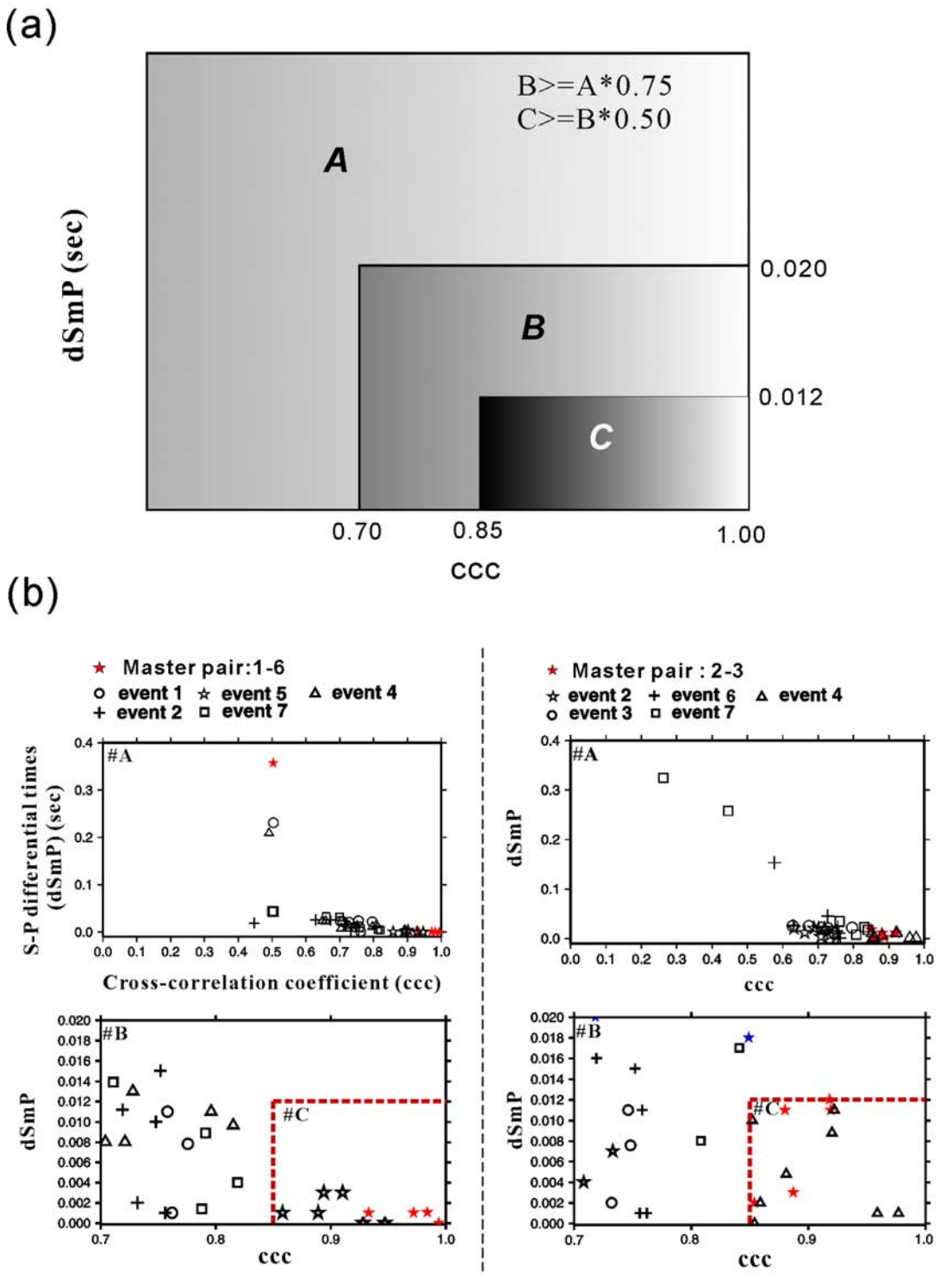

Figure 3. (a) Schematic illustration of the composite criteria used for repeating earthquake identification in the study area. (b) The ccc, dS_mP statistics for an example group of similar events compared with (left) event 1 and (right) event 2. (bottom) Each point maps the dS_mP and ccc for an event pair at a single station. Points with identified symbols are for the same event paired with the master pair. (top) Zoom of the area with ccc $\geq$ 0.85 and $dS_mP \leq 0.012$ s. In Figure 3b (top left), event 5 passes the selected criteria discussed in the text and therefore is grouped into a repeating sequence with events 1 and 6. In Figure 3b (top right), event 4 passes the selected criteria and is grouped into a repeating sequence with events 2 and 3.

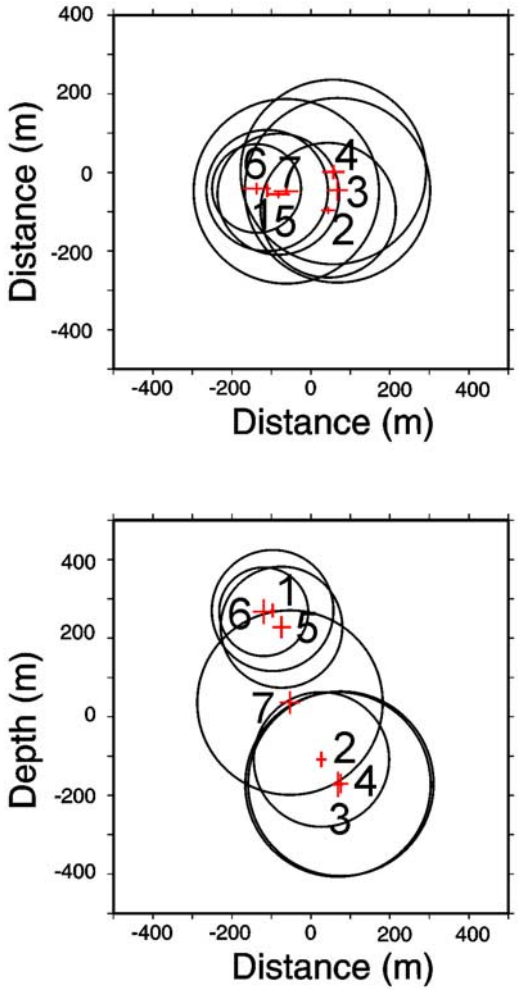

Figure 4. HypoDD relocation results separate the Figure 3 event group into two real repeating sequences, events 1-5-6 and events 2-3-4.

inaccurate origin times and interstation timing. The repeating event identification scheme has been detailed by *Chen et al.* [2008] and will be only briefly outlined below.

[9] An illustration of the method of composite selection criteria is shown in Figure 3. We populate the [dS_mP, ccc] space with similarity point measurements (dS_mP, ccc) where each point represents the dS_mP and ccc measurements between two events for a given station. All event pair combinations for a similar event group are considered. We break the similarity space into three regions (A, B, and C). Region A is the area for overall measurements, region B is the area of ccc $\geq$ 0.70 and $dS_mP \leq 0.02$ s, and region C is the area of ccc $\geq$ 0.85 and $dS_mP \leq 0.012$ s. Region A encompasses regions B and C, and region B includes region C. For two events to be considered a repeating pair, at least 75% of their similarity points must lie within region B, and of those points at least 50% must also lie within region C. Once repeating pairs have been selected, they are organized into repeating event sequences. Each sequence is a collection of events linked by the composite criteria to at least one other member of the sequence. The criteria have been determined on the basis of empirical testing using a subset of the event pairs where sufficient data quantity and quality exist for confirmation of patch rerupture through earthquake relocation.

[10] Figure 3b shows an example of ccc, dS_mP statistics for a group of similar events whose waveform cross correlations are greater than 0.70 and magnitudes range from 2.8 to 3.5. On the basis of the composite selection criteria, events 1, 5, and 6 are grouped into a subgroup, whereas events 2, 3, and 4 are grouped into a different subgroup. Double-difference earthquake relocation (HypoDD [*Waldhauser and Ellsworth*, 2000]) of this similar event group using waveform cross-correlation time delay estimates is shown in Figure 4. Relocation results separate this event group into two repeating sequences, events 1-5-6 and events 2-3-4, agreeing with the subgroups identified by the composite selection criteria.

[11] Additional tests using other similar event clusters reveal that the exclusion of events by HypoDD and the timing and associated relative location errors occur occasionally for the study area. These errors, in conjunction with the sparse and one-sided coverage of the Central Weather Bureau Seismic Network (CWBSN) stations, intermittent station outages for the sparse network, and the temporally unstable noise characteristics of the CWBSN records, make systematic identification of repeating events using a location-based approach impractical. The composite selection approach has an obvious advantage in areas with poor station coverage and low SNR.

4. Similarity and Variability in RES's Behavior

[12] Approximate 9000 earthquakes (M 1.9 to 6.5) recorded by the CWBSN from 1991 until 2004 have been used for a repeating earthquake search in the study area [*Rau et al.*, 2007; *Chen et al.*, 2008]. Magnitude statistics indicate that the CWBSN catalog is complete for magnitudes as low as M_L 1.9. Seismograms for the events were recorded by the short-period CWBSN stations at sampling rates of 50, 100, and 200 Hz, with the rate depending on the time period of data acquisition. For this study, we have used vertical component seismograms from at least seven CWBSN stations having relatively low noise levels (solid triangles in Figure S1 in the auxiliary material[1]). Figure 5 shows the nearly identical waveforms for a RES example (H24 in Table 1). Using the composite selection criteria, we have identified 58 RES containing 215 repeating events in eastern Taiwan.

4.1. Spatial Characteristics of RES

[13] The RES are found in the areas of relatively high seismic activity, as shown by the yellow and orange colors in Figure 1b (X, Y, and Z). Area X lies near the north end of the Longitudinal Valley, close to Hualien city, extending offshore to the subduction zone in northern Taiwan. Area Y is located to the west of area X, underneath the eastern flank of the Central Range. Area Z is near the town of Chihshang in the southern portion of the LVF. Note that RES are observed only in areas Y and Z. The main reason we did not find RES in area most earthquakes being located offshore with relatively high noise levels. Because of low data quality, the distinction between repeated and nonrepeated

[1] Auxiliary materials are available in the HTML. doi:10.1029/2007JB005518.

Table 1. Repeating Earthquake Sequences in Eastern Taiwan[a]

ID	N	Longitude (deg)	Latitude (deg)	Depth (km)	M_L	T_r (years)	Slip Rate (cm/a)	COV in M_0	COV in T_r	Duration (years)	Type
H1	4	121.475	23.897	18.86	2.7–2.8	0.59–0.86	3.09	0.13	0.18	2.32	B
H2	3	121.451	23.918	16.41	2.700	1.86–3.30	2.23	0.00	0.28	5.17	Ap
H3	3	121.490	23.903	18.37	3.1–3.2	0.92–0.95	2.81	0.16	0.01	1.87	B
H4	3	121.462	23.929	20.42	2.8–2.9	1.26–4.68	2.44	0.14	0.58	5.95	Ap
H5	6	121.467	23.961	14.95	2.5–2.6	0.81–2.06	4.19	0.11	0.41	6.09	Ap
H6	3	121.475	23.948	14.29	2.7–2.8	0.54–0.54	2.27	0.16	0.00	1.09	B
H7	3	121.495	23.922	20.11	2.6–3.2	0.41–8.69	3.47	0.59	1.17	9.84	Ap
H8	4	121.464	23.858	17.26	2.9–3.0	0.06–0.20	3.40	0.16	0.47	0.38	B
H9	5	121.483	23.961	17.45	2.5–2.7	0.91–2.73	3.52	0.28	0.53	6.39	Ap
H10	3	121.465	23.943	14.38	2.900	2.47–2.68	2.48	0.00	0.04	5.15	Qp
H11	3	121.401	23.724	17.31	2.7–2.8	1.82–2.05	2.31	0.14	0.06	3.87	Qp
H12	3	121.453	23.919	18.34	2.1–2.4	1.16–1.23	1.74	0.41	0.03	2.39	B
H13	3	121.426	23.857	17.00	2.9–3.0	1.23–3.22	2.53	0.16	0.45	4.46	Ap
H14	4	121.420	23.682	10.05	2.4–2.7	0.64–1.95	2.79	0.38	0.41	3.88	Ap
H15	3	121.484	23.947	20.04	3.1–3.2	1.66–2.71	2.86	0.14	0.24	4.37	Qp
H16	4	121.434	23.714	17.97	3.2–3.3	1.48–3.52	3.93	0.15	0.57	6.81	Ap
H17	3	121.431	23.825	18.79	2.7–2.9	1.63–1.91	2.31	0.32	0.08	3.54	Qp
H18	4	121.501	23.939	16.99	3.7–3.9	2.32–3.20	**5.28**	0.25	0.09	5.87	Qp
H19	3	121.474	23.939	17.61	2.1–2.6	0.51–2.64	1.84	0.64	0.68	3.16	Ap
H20	5	121.434	23.698	12.07	2.8–3.3	<0.01–2.86	4.62	0.43	0.62	5.26	Ap
H21	5	121.468	23.721	17.11	3.8–3.9	2.09–3.74	**6.91**	0.14	0.04	5.05	Qp
H22	4	121.515	24.037	19.89	2.3–2.6	0.8–1.9	2.60	0.34	0.33	4.59	Ap
H23	3	121.499	24.034	20.60	2.7–2.8	1.9–2.2	2.27	0.15	0.49	4.11	Ap
H24	6	121.524	24.086	21.86	2.3–2.6	<0.01–3.48	3.90	0.30	1.25	6.38	Ap
H25	5	121.526	24.074	20.78	4.5–4.7	2.4–4.3	**8.04**	0.17	0.21	13.09	Qp
CH1	3	121.384	23.132	16.93	2.2–2.8	1.2–4.3	1.80	0.25	0.56	5.54	Ap
CH2	5	121.394	23.144	18.19	1.9–2.9	1.0–2.5	3.56	0.69	0.32	7.11	Ap
CH3	3	121.368	23.156	12.61	2.8–2.9	1.8–6.1	2.39	0.53	0.55	7.86	Ap
CH4	4	121.393	23.146	17.60	2.8–3	1.0–2.5	3.22	0.54	0.41	5.04	Ap
CH5	4	121.395	23.150	18.04	2.9–3.2	1.8–4.1	3.74	0.32	0.46	9.03	Ap
CH6	5	121.399	23.153	18.74	2.5–2.8	0.1–3.2	3.68	0.32	0.85	5.90	Ap
CH7	3	121.399	23.174	17.60	2.5–3.0	3.0–5.7	2.32	0.56	0.31	8.77	Ap
CH8	3	121.401	23.150	18.72	2.5–2.8	2.6–4.5	2.23	0.36	0.28	7.14	Ap
CH9	3	121.376	23.153	19.89	3.2–3.6	2.8–5.4	3.37	0.44	0.32	8.18	Ap
CH10	3	121.377	23.134	17.00	2.4–2.8	3.20	2.20	0.12	0.00	6.33	Qp
CH11	3	121.377	23.125	16.74	2.7–3.7	1.8–5.0	3.15	0.74	0.47	6.78	Ap
CH12	3	121.374	23.208	12.74	2.1–2.3	2.7–4.4	1.71	0.25	0.24	7.04	Qp
CH13	3	121.435	23.150	22.55	2.1–2.9	0.8–2.6	2.16	0.63	0.54	3.44	Ap
CH14	3	121.426	23.161	21.19	2.5–2.8	2.5–3.3	2.20	0.34	0.13	7.42	Qp
CH15	3	121.404	23.162	19.70	2.6–2.7	1.3–4.1	2.17	0.18	0.31	3.75	Ap
CH16	3	121.389	23.230	13.48	2.1–2.2	1.6–1.7	1.69	0.21	0.01	3.27	Qp
CH17	4	121.336	23.164	7.09	2.1–2.3	1.8–2.9	2.31	0.24	0.21	7.55	Qp
CH18	4	121.413	23.153	10.88	2.1–3.0	1.0–4.0	3.02	0.59	1.00	6.42	Ap
CH19	3	121.384	23.197	13.89	2.0–2.3	1.4–3.8	1.70	0.31	0.46	5.20	Ap
CH20	5	121.438	23.157	21.67	2.5–2.6	1.2–2.4	3.43	0.26	0.30	7.67	Ap
CH21	7	121.376	23.133	16.20	2.0–2.4	<0.01–4.0	3.90	0.45	1.75	5.01	Ap
CH22	3	121.410	23.214	20.59	2.1–2.3	0.4–1.4	1.71	0.25	0.53	1.84	B
CH23	3	121.336	23.164	7.09	2.1–2.3	1.8–2.9	1.71	0.25	0.24	4.74	Qp
CH24	4	121.402	23.179	17.87	2.0–3.0	1.2–3.9	2.80	0.93	0.63	6.64	Ap
CH25	3	121.404	23.156	19.41	2.3–2.5	2.0–3.1	1.94	0.26	0.21	5.17	Qp
CH26	3	121.396	23.163	18.22	2.5–3.0	2.6–3.0	2.24	0.72	0.07	5.56	Qp
CH27	4	121.404	23.163	19.70	2.6–2.7	0.4–2.5	2.86	0.15	0.44	4.19	Ap
CH28	4	121.364	23.151	12.85	2.3–2.5	1.6–3.1	2.50	0.27	0.27	7.05	Ap
CH29	4	121.335	23.105	11.96	2.5–2.8	2.2–3.1	2.82	0.43	0.18	8.27	Qp
CH30	5	121.373	23.160	15.34	2.1–3.0	1.2–3.4	3.65	0.73	0.38	8.50	Ap
TT1	3	121.242	22.938	22.73	2.0–3.0	<0.001	1.92	1.09	0.57	0.1	B
TT2	4	121.319	22.894	20.31	2.3–2.5	1.0–6.6	2.60	0.23	0.69	10.2	Ap
TT3	3	121.086	22.854	12.86	2.6–2.9	3.6–5.1	2.27	0.41	0.17	8.66	Qp

[a]H, CH, and TT represent Hualien, Chihshang, and Taitung repeating earthquake sequence clusters, respectively. Duration is the lifetime of a sequence. T_r is the recurrence interval of each sequence. Slip rate is long-term creep rate measured by equation (2). COV in T_r and COV in M_0 are the coefficient of variation in recurrence interval and seismic moment, respectively. B, Ap, and Qp indicate burst-type, aperiodic, and quasiperiodic repeating sequences, respectively.

event statistics is less clear and therefore, the RES identifications less confident in area X.

[14] In area Y, referred to as the "Hualien segment," we have identified 25 M 2.3–4.6 RES containing 95 repeating events: the "Hualien RES cluster" [*Rau et al.*, 2007]. This cluster occurred on a 45-km-long fault patch (23.70°N to 24.09°N in Figure 1) at a depth of 10–22 km. In area Z, referred to as the "Chihshang segment," we have defined 30 M 2.1–3.4 RES containing 110 repeating events occurring on a 15-km-long fault patch at 7–23 km depth [*Chen et al.*, 2008]. This group of repeating events, "Chihshang RES cluster," tends to be concentrated on the northern portion of the Chihshang fault, which is the most active segment along the LVF. In the southern end of the LVF near Taitung city,

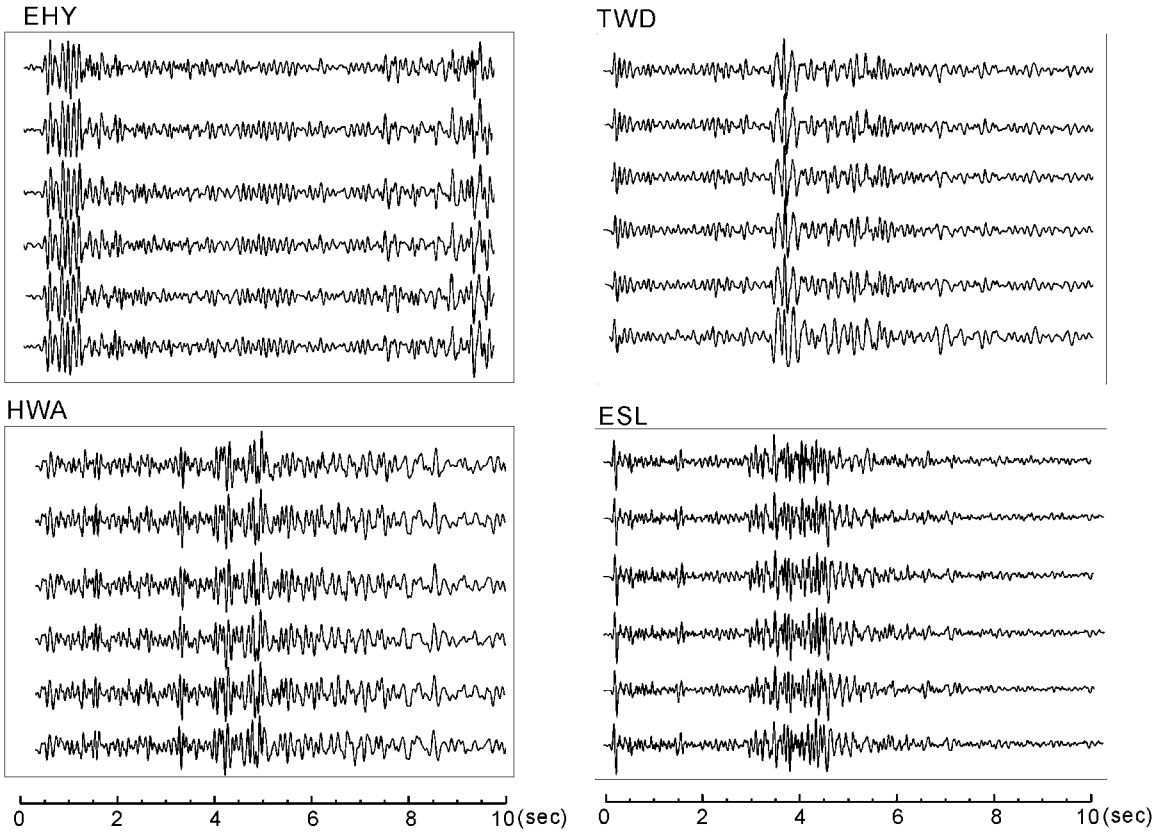

Figure 5. Filtered 2–18 Hz waveforms recorded at stations EHY, HWA, TWD, and ESL from an example of a repeating sequence (M 2.6). Each trace is normalized by its maximum amplitude.

three sparsely distributed RES are found with a magnitude range of 2.4–2.8. Because of the limited number of RES and their unknown relation to the nearby fault zone, these Taitung RES will not be discussed further here. The parameters for each RES are listed in Table 1. In Figure 2 we have superimposed the locations of the repeating earthquake sequences on the fault model derived from *Kuochen et al.* [2004]. Note that on the Hualien segment, most of the RES occur at the junction of the subducting EP and the west dipping PSP (Figure 2a), whereas on the Chihshang segment, RES occur along the east dipping fault plane (Figure 2b).

4.2. Temporal Characteristics of RES

[15] On the basis of the occurrence lifetime (i.e., duration) and regularity in the recurrence time, we classify the repeating sequences into three different types. The sequences with repeating events that are active only for a short period of time (i.e., 3 years in this study) are classified as ''burst-type'' repeating sequences (B type), whereas those sequences with durations longer than 3 years are defined as ''nonburst-type'' repeating sequences (non-B type). Non-B-type sequences are further separated into ''quasiperiodic'' and ''aperiodic'' sequences based on the variation in recurrence times between events in a sequence, as represented by the coefficient of variation (COV, standard deviation divided by the mean). A COV of 0 implies perfect periodicity, COV $\cong$ 1 implies Poissonian recurrence, and COV > 1 indicates temporal clustering. Here we use a COV in recurrence interval (COV_{Tr}) value of 0.25 as the threshold to separate quasiperiodic (Qp type) from aperiodic-type (Ap type) sequences.

[16] In Figure 6a we show that the Hualien RES cluster is characterized by a larger magnitude range than the Chihshang RES cluster. The event number in each RES ranges from 3 to 7 and from 3 to 6 for Chihshang and Hualien RES clusters, respectively. COV as a function of each RES's magnitude is shown in Figure 6b, which illustrates that the COVs in both recurrence interval and seismic moment are confined to less than 0.3 for the $M \geq 3.8$ RES. This implies that large repeating events ($M \geq 3.8$) tend to recur in a more regular manner and with more uniform size. When the event size decreases, the range of variations in regularity and size becomes larger, indicating a more complicated recurrence behavior for smaller RES. We also note that $M \geq 3.8$ RES have not yet been found on the Chihshang segment.

[17] In Figures 7a and 7b we compare the characteristics of the RES' regularity in time and size. About 52% of the Hualien and 67% of the Chihshang RES clusters exhibit aperiodicity (i.e., RES with $COV_{Tr} \geq 0.25$), respectively. In Figure 7b, the histogram of COV in seismic moment (COV_{M0}) shows that the events in each sequence of the Hualien RES cluster appear slightly more uniform in size than those in the Chihshang RES cluster. The subtle difference in recurrence behavior (i.e., regularity in event size and timing) between the two fault segments implies that the regional loading condition and its temporal variation may vary little.

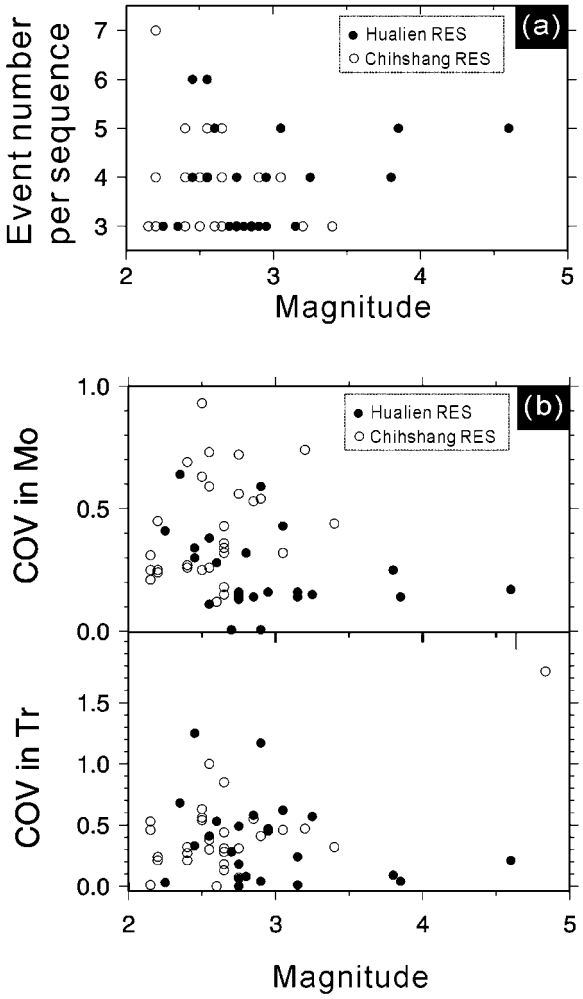

Figure 6. (a) Average magnitude versus event number of each RES. (b) Average magnitude of each RES versus the COV in (top) seismic moment and (bottom) recurrence interval for Chihshang and Hualien RES clusters.

[18] In Figure 7c we compare the characteristics of RES duration for the Hualien and Chihshang RES clusters. The durations range from 0.38 to 13.1 years and 1.84 to 9.03 years for sequences in the Hualien and Chihshang RES clusters, respectively. In the Hualien RES cluster, five sequences have a short occurrence lifetime (i.e., B type), whereas in the Chihshang RES cluster, only one sequence is of a B type. We find that these B-type sequences are not spatially adjacent to each other. Their spatial separation ranges from 1 to 12 km, where the shortest separation, 1 km, is about 7.5 times the rupture dimension of a M 3.1 repeating event. We also observe that some B-type sequences start or shut down after nearby M 5 events. This temporal correspondence, however, does not always appear when the repeaters are in the vicinity of M 5 events.

[19] The same type of RES has also been found in Japan subduction zones and Central California [*Igarashi et al.*, 2003; *Kimura et al.*, 2006; *Templeton et al.*, 2008], where the proposed mechanisms are variable creep rate in the surrounding cavity (area between asperities). The change in creep rate may be associated with local fluctuations in stress from larger nearby earthquakes and aseismic slip from episodic slow slip or continuous secular motion. Long-duration RES likely indicate that creep in the surrounding area is occurring more steadily over the observation period [e.g., *Templeton et al.*, 2008]. In eastern Taiwan, the limited

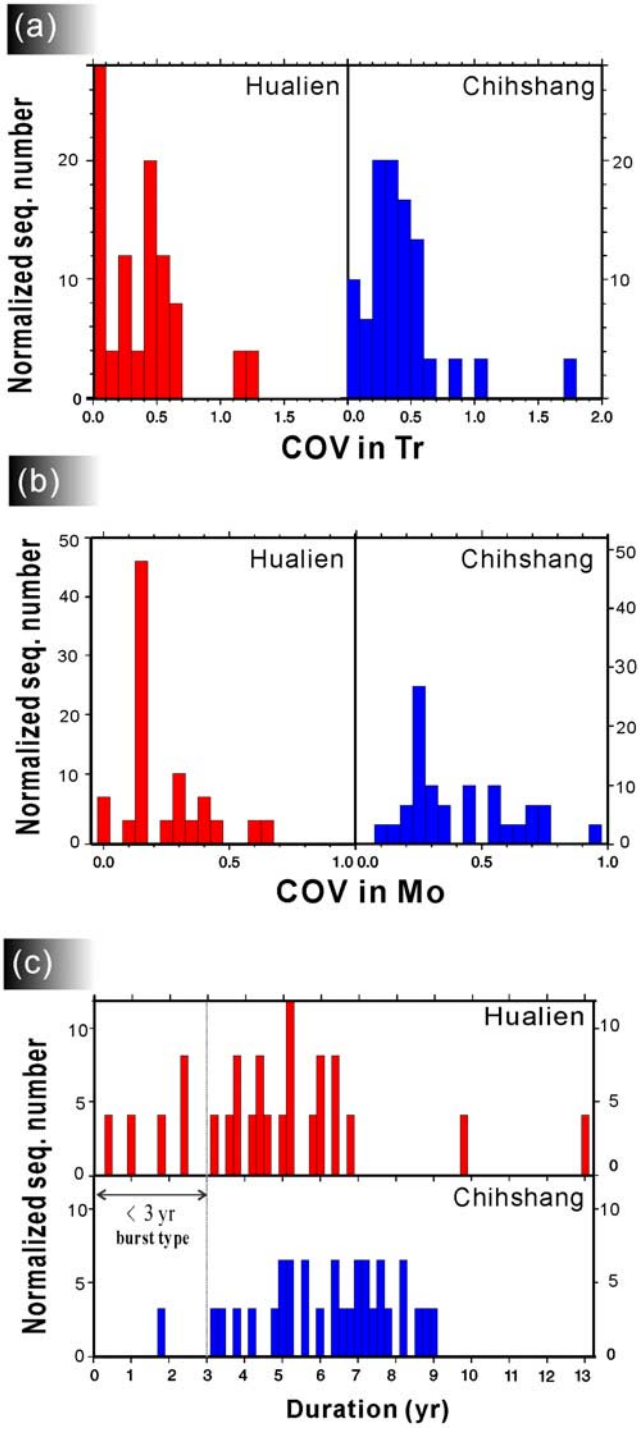

Figure 7. (a) COV in recurrence interval, (b) COV in seismic moment, and (c) occurrence lifetime (duration) as a function of normalized sequence number for the Hualien and Chihshang repeating clusters. The normalized number is calculated by the proportion to the overall repeating sequences in that area.

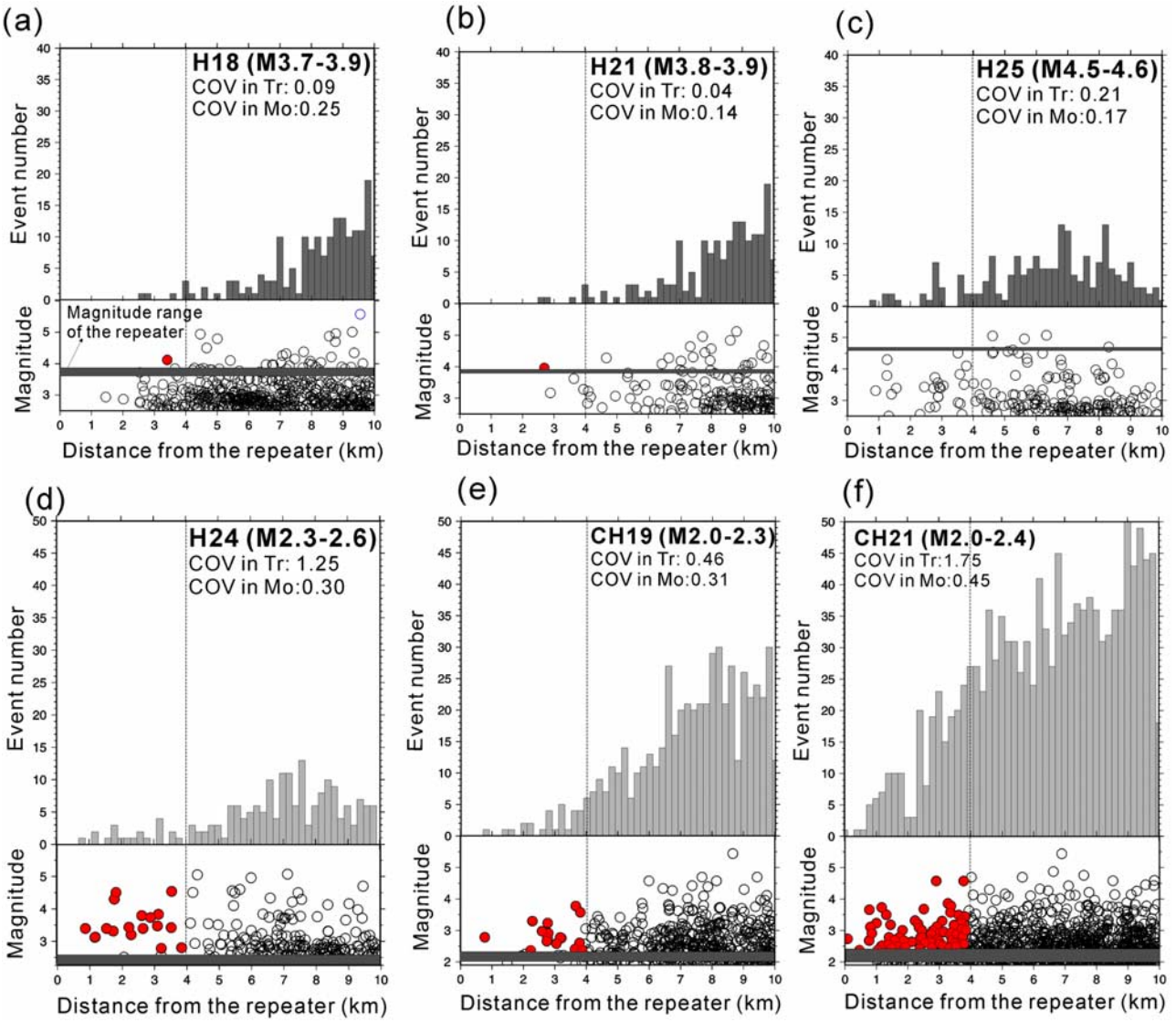

Figure 8. (top) Number and (bottom) size of earthquakes adjacent to the target RES (a) H18, (b) H21, (c) H25, (d) H24, (e) CH19, and (f) CH21. Horizontal gray box denotes the magnitude range of the target RES. Earthquakes located within 4 km of the target RES with greater magnitude than the RES are highlighted in red circles. Detailed information for each RES is shown in Table 1.

number of B-type RES and sparse information regarding the possible slow earthquakes and temporal changes in fault zone properties complicate our understanding of the cause of B-type sequences. Further updates of repeating earthquake data in the study area and a comparison with temporal variations in geodetically derived slip rate are planned.

5. Influence of Neighboring Events on RES's Regularity

[20] Simulations of the interaction between asperities suggest that stress perturbations caused by nearby events can complicate earthquake recurrence, whereas regularity is more evident in spatially isolated asperity systems [e.g., *Kato*, 2004; *Ariyoshi et al.*, 2007]. *Lynch et al.* [2003] modeled the interaction between event sequences on two rupture segments separated by an intervening creeping fault segment, and showed that event separation, the viscosity of the lower crust, and differences in average recurrence intervals of the two fault segments strongly influence the event recurrence patterns. Natural systems exhibit some of the model-predicted recurrence properties. The detailed record of repeating microearthquakes reveals that the regularity of earthquake recurrence is controlled by the stress perturbations from nearby larger events and the distance between events [*Chen et al.*, 2007a]. Therefore, in this section we discuss how background earthquakes influence nearby RES and their recurrence patterns.

[21] A measure of the number and size of neighboring earthquakes is plotted against the separation distance (i.e., the distance from an RES to a non-RES earthquake in the vicinity) for six representative RES in Figure 8. The $M \geq 3.8$ quasiperiodic RES are commonly surrounded by low seismic activity within a distance of 4 km; the neighboring events are

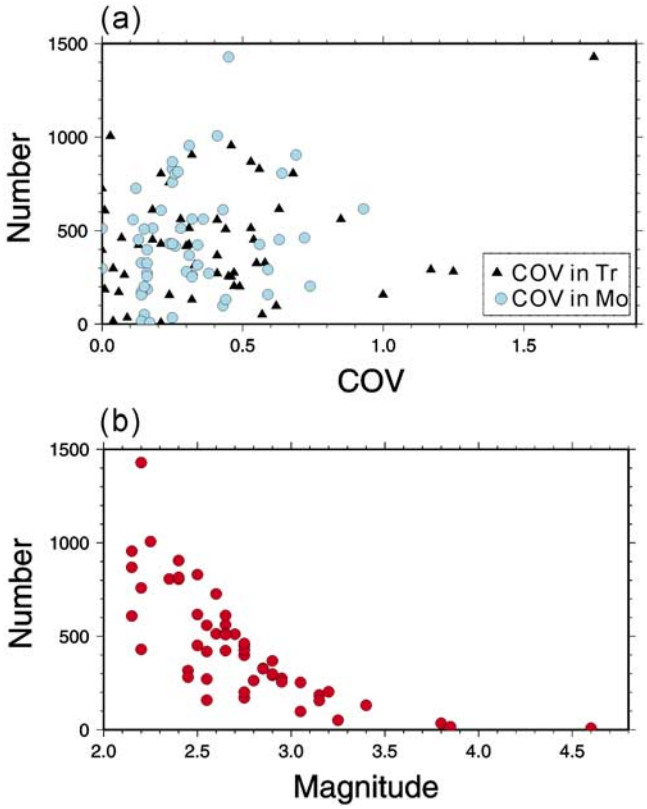

Figure 9. (a) COV in recurrence interval (triangle) and seismic moment (circle) of the 55 RES versus number of neighboring earthquakes within a distance of 10 km. (b) RES magnitude versus number of neighboring earthquakes within a distance of 10 km. Note that only the earthquakes with larger magnitude than the target repeater are presented.

mostly smaller than the RES in size (Figures 8a–8c). The examples in Figures 8d and 8e illustrate that with a larger number of bigger earthquakes nearby, the smaller-magnitude RES recur in a more irregular manner ($COV_{Tr} \geq 0.5$). Figure 8f shows a small magnitude RES surrounded by high earthquake activity having a COV_{Tr} up to 1.75, where the size variability (COV_{M0}) is as large as 0.45. These examples imply that both the size and number of the background earthquakes adjacent to a RES have a large impact on its recurrence. Fewer neighboring larger-sized earthquakes likely facilitate quasiperiodic recurrence of a RES. Moreover, the influence of neighboring events not only affects the regularity of the recurrence time but also the uniformity of the repeater's size.

[22] We have also examined the relationship between all of the 55 RES and their nearby nonrepeating events. We observe that 16 RES are surrounded by low earthquake activity in the vicinity; that is, within a distance of 4 km, there are fewer than 5 nonrepeating events calculated for every 0.1 km. Most of these 16 RES exhibit a quasiperiodic pattern ($COV_{Tr} \leq 0.25$), whereas 5 of the 16 RES are aperiodic sequences that are either $M \leq 2.5$ and/or surrounded by $M \geq 4$ events within a 2 km distance. In Figure 9a we show that there is no obvious systematic trend of COV_{Tr} and COV_{M0} decreasing with increasing RES size or with decreasing number of surrounding events. Several small RES in zones of high seismic activity still exhibit a quasiperiodic behavior. This suggests that the factors controlling the recurrence properties of small RES are complicated and cannot be fully answered in the current study. In Figure 9b, however, there exists a systematic trend in RES's magnitude with the density of larger-sized neighboring events. With increasing magnitude of the RES, fewer larger-sized earthquakes are seen to occur in the vicinity, which likely causes less influence on the RES's timing and therefore leads to more regular recurrence.

[23] The salient features of RES, however, can be summarized as follows: (1) A relatively large RES (e.g., $M \geq 3.8$) is less influenced by nearby earthquake activity and therefore recurs in a regular manner; and (2) small RES may be influenced by nearby earthquakes more easily, and the factors controlling RES behavior are more complicated. The COV_{Tr} can be less than 0.25 for RES surrounded by a large number of earthquakes, while its COV_{M0} is large (e.g., $COV_{M0} = 0.45$). Spatially isolated small RES, on the other hand, do not always reveal quasiperiodic patterns and uniform size. These facts indicate that for the small RES, the number and size of the adjacent earthquakes cannot completely account for the recurrence characteristics.

6. Discussion

6.1. Spatial Extent of RES on the Two Segments and Deep Fault Behavior

[24] Numerical, analytical, and laboratory experiments suggest that steady aseismic creep in the region surrounding the RES is required to drive the repeated ruptures [*Sammis et al.*, 1999; *Anooshehpoor and Brune*, 2001; *Beeler et al.*, 2001; *Johnson and Nadeau*, 2002]. This is in agreement with the large number of RES observed on creeping fault segments [*Vidale et al.*, 1994; *Nadeau et al.*, 1995; *Nadeau and McEvilly*, 1999; *Rubin et al.*, 1999; *Matsuzawa et al.*, 2002; *Uchida et al.*, 2003; *Nadeau and McEvilly*, 2004]. It is generally accepted that repeating events are located on the edge of or far from larger asperities and are caused by repetitive rupture of small asperities surrounded by stable sliding areas [*Beeler et al.*, 2001; *Sammis and Rice*, 2001; *Johnson and Nadeau*, 2002; *Nadeau and McEvilly*, 2004]. Regions of seismically active but nonrepeating events could be either weakly coupled (i.e., creeping, low level of friction) or strongly coupled (i.e., locked, which generate large amplitudes of slip coseismically). In Parkfield, the transition from locked to creeping behavior is shown by along-strike variation of surface slip rates, which can be well correlated with the slip rates derived from repeating earthquakes [*Nadeau and McEvilly*, 1999].

[25] At the focal depth of 10–25 km where the repeating events are found, the Chihshang RES cluster is confined to a narrow range of 15 km along the strike of the fault. Prior studies indicate that the northern section of the Chihshang segment (north of 23.1°N) where the 30 RES took place, is likely a weakly coupled area because the 3 cm/a averaged slip rate at depth is comparable to the surface rate [*Chen and Rau*, 2003]. We interpret the northern deeper section of the Chihshang segment, encompassing the RES and active seismicity, as a stable-sliding area. Notably the subsequent 2003 M_L 6.4 main shock occurred at the boundary where the repeaters stop, and its aftershocks propagated southward to

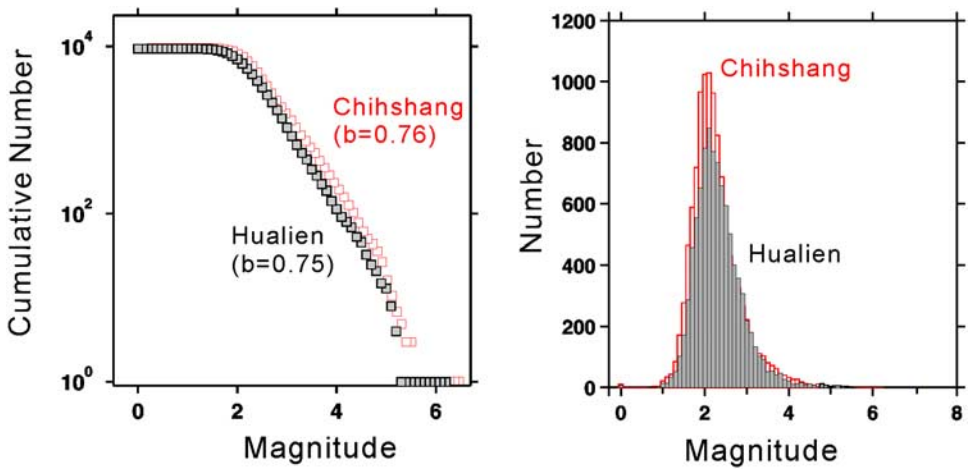

Figure 10. (left) Frequency-magnitude distribution and (right) event magnitude histogram for 1991–2004 seismicity in the Chihshang (red open symbols) and Hualien areas (gray filled symbols).

avoid this section. Geodetically derived slip distribution of the 2003 M_L 6.4 event indicates that the coseismic slip zone concentrates in the southern deeper section of the fault [*Ching et al.*, 2007; *Hu et al.*, 2007]. This implies that during the study period of 1991–2003 December (prior to the M_L 6.4 earthquake) fault creep may have been restricted to the northern deeper section of the Chihshang segment. The deeper southern section, where the major slip of a subsequent M_L 6.4 event occurred, is inferred as a strongly coupled area.

[26] In contrast to the localized RES on the northern Chihshang segment, the Hualien RES span the entire length of the fault zone with a spatial extent of 45 km in a NNE direction, where the fault zone is identified by the seismicity cluster underneath the eastern flank of the Central Range. Unlike the well-documented creep rate studies on the Chihshang fault [*Yu and Liu*, 1989; *Angelier et al.*, 2000; *Lee et al.*, 2003], the geodetically derived deep fault deformation in the Hualien RES zone is lacking. The RES observation in this zone suggests that localized aseismic slip is occurring at depth. With a similar depth range, the spatial distribution of RES on the Chihshang and Hualien segments may imply the distinct spatial extent of the deep creeping zone. At the deeper part of the fault where the most seismicity occurs, the Hualien segment is likely characterized by a wider distributed aseismic slip area than that on the Chihshang segment.

6.2. Absence of $M \geq 3.8$ RES on the Chihshang Segment

[27] While the Hualien segment produces M 3.8–4.6 RES, the Chihshang segment only produces $M < 3.5$ RES. This fact raises several questions: what causes the Hualien RES' magnitudes to be much larger than those of the Chihshang RES? Is the fault zone heterogeneity responsible for the absence of $M \geq 3.8$ RES in the Chihshang segment? Is the stress loading rate in the Chihshang segment too slow to observe large RES during the study period? Are there other factors associated with fault properties may impact the size limit of RES? Below, we propose possible factors that may be responsible for the lack of $M \geq 3.8$ RES on the Chihshang segment.

6.2.1. Lack of Comparable Size Asperities on the Fault

[28] *Lay and Kanamori* [1980] and *Astiz and Kanamori* [1984] argued that a regional distribution of comparable large-sized asperities on the fault contact plane may have been responsible for the frequent occurrence of M 6–7 doublets in the Mexican subduction area. Simulations on the fault systems show that strong fault heterogeneity leads to complex slip patterns and a wide range of event sizes [*Ben-Zion and Rice*, 1995], where they suggested that in a system characterized by a narrow range of geometric disorder, earthquakes reaching the critical size become unstoppable and continue to grow to a size limited by a characteristic system dimension. Conversely, in a system characterized by a broad range of geometric disorder, a correspondingly broad spectrum of critical event sizes exists. *Wang and Huang* [2006] investigated the effects of fault zone roughness on the characteristics of long-term seismicity using numerical simulation, and showed that a lower fault roughness leads to greater likelihood of generating large earthquakes.

[29] Fault zone heterogeneity, exhibited by the asperity distribution, can be studied through frequency-size statistics of earthquakes [e.g., *Turcotte*, 1989; *Ben-Zion and Rice*, 1993, 1995]. The frequency-magnitude distribution of earthquakes on the Chihshang and Hualien segments may vary, which implies that the missing $M \geq 3.8$ RES are due to a lack of comparably sized ($M \geq 3.8$) asperities on the Chihshang segment. In Figure 10, the frequency-magnitude distribution of earthquakes parameterized by the b value, however, reveals similar values (0.75 and 0.76) for the two segments. The event magnitude histograms for the two regions also reveal a similar peak at $M = 2.2$ (Figure 10). This indicates that the frequency-magnitude distribution of earthquakes in these two regions varies little and therefore will unlikely play a significant role in determining the absence of $M \geq 3.8$ RES in the Chihshang segment.

6.2.2. Fault Loading Rate

[30] The recurrence interval of repeating earthquakes is thought to be inversely proportional to the loading rate on a fault [e.g., *Scholz*, 1990; *Schaff et al.*, 1998; *Nadeau and Johnson*, 1998; *Nadeau and McEvilly*, 1999; *Beeler et al.*,

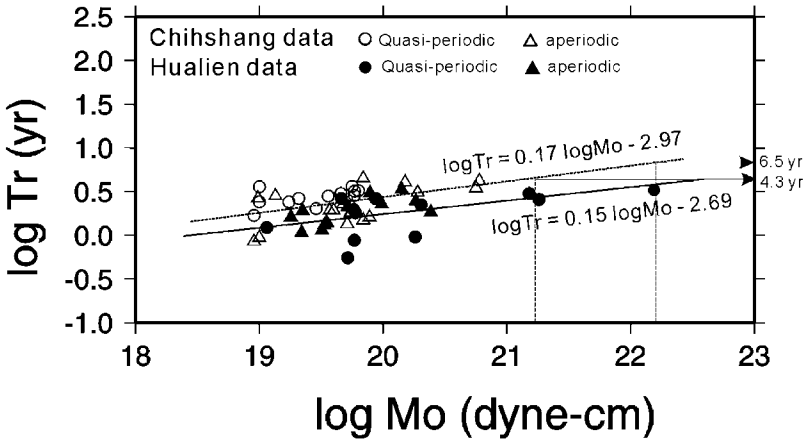

Figure 11. Recurrence interval as a function of seismic moment. Circles and triangles represent the quasiperiodic (COV in recurrence interval ≤ 0.25) and aperiodic (COV in recurrence interval ≥ 0.25) RES, respectively. Scaling line is linear least squares fit with slope 0.17 and 0.15 for the Chihshang and Hualien RES clusters, respectively.

2001]. For example, on the Hayward fault, which that creeps at 5 mm/a, $M \geq 3$ repeating earthquakes have not yet been found [*Bürgmann et al.*, 2000]. In comparison, in the creeping section on the San Andreas fault, which has a 2.3 cm/a creep rate, $M \geq 3$ repeating earthquakes exist at Parkfield [*Nadeau et al.*, 1995; *Nadeau and McEvilly*, 1999, 2004]. The observed repeating event's magnitude, therefore, is primarily a function of fault slip rate and observation period.

[31] A slow fault loading rate may lead to a longer recurrence interval in repeating sequences, and therefore might not be detected in the 13-year observation period. The GPS-determined slip rate for the Hualien and Chihshang segments is estimated to be 4.75 ± 0.58 cm/a at 15–25 km depth [*Rau et al.*, 2007] and 3.7–4.2 cm/a at 10–20 km depth [*Johnson et al.*, 2005], indicating similar slip rate values. Such a slight difference in loading rate for the Chihshang segment is not likely responsible for the lower event magnitude on this fault segment.

[32] It remains unclear how exactly the difference in fault slip rate affects the recurrence interval. *Chen et al.* [2007b] addressed the influence of the regional loading rate on RES recurrence using repeating earthquake data from three distinct tectonic settings: the San Andreas fault, the Japan subduction zone, and a creeping oblique fault in eastern Taiwan. The difference in intercept is revealed on a log-log plot of average recurrence interval (T_r) against the average seismic moment (M_0) represents the difference in fault loading rate. The T_r-M_0 relation is remarkably consistent among the three regions when adjusted to account for differences in the geodetically derived slip rates.

[33] In Figure 11 we show the T_r-M_0 relation from the Hualien and Chihshang RES clusters, respectively. There appears to be a weak linear relationship in log-log space between recurrence interval and seismic moment. The recurrence interval for the RES on the Hualien segment is ~3/4 times shorter than that observed on the Chihshang segment, suggesting its ~3/4 higher fault slip rate. This result is consistent with the GPS-derived slip rates. Given the T_r-M_0 scaling for the Chihshang RES cluster, the M 3.8 and M 4.6 events are expected to recur at intervals of 4.4 and 6.5 years, respectively, which are longer than the 3.1 and 4.3 year intervals calculated for the Hualien RES cluster. The expected recurrence interval for a M 3.8 RES on the Chihshang segment (if any) is short enough to be detected during the study period. Therefore, we conclude that the lower fault loading rate will not likely explain the lack of $M \geq 3.8$ RES on the Chihshang segment.

6.2.3. Isolation From Nearby Larger Repeating Events

[34] A regional distribution of comparably sized asperities may be responsible for the occurrence of RES and for their recurrence regularity. Simulations of earthquake interactions explore the importance of stress fluctuations from nearby earthquakes on the timing and regularity of earthquake recurrence [e.g., *Kato*, 2004; *Ariyoshi et al.*, 2007]. In natural fault systems, the earthquake interaction pattern (Figure 8) indicates that spatial isolation is the key to regularity in RES. Repeating microearthquakes at Parkfield, California show that more isolated earthquakes occur in a more regular manner [*Chen et al.*, 2007a].

[35] Since all the $M \geq 3.8$ RES exhibit quasiperiodic behavior, the RES's regularity and the existence of larger RES are probably explained by the same mechanisms. We therefore infer a possible scenario on an asperity model illustrating how the spatial isolation of earthquakes explains the absence of relatively large RES ($M \sim 4$ or larger) on the Chihshang segment. As shown in Figures 12a and 12b, open patches represent the location of asperities, and larger patches represent relatively large earthquakes ($M \sim 4$ or larger). The asperities are surrounded by aseismic slip regions as denoted by 'creeping area'. The distance between $M \sim 4$ asperities is probably much shorter on the Chihshang segment then on the Hualien segment, which represents the difference in the $M \sim 4$ asperity's isolation between the two segments. When seismic slip occurs at one asperity, post-seismic sliding following the earthquake may propagate in the vicinity, reach another asperity and trigger rupture. The triggering behavior is insignificant when the seismic slip is slow; therefore large events would be less perturbed by stress changes from small nearby events. On the Chihshang segment neighboring asperities are separated by a narrow region of stable-sliding frictional properties, thus the inter-

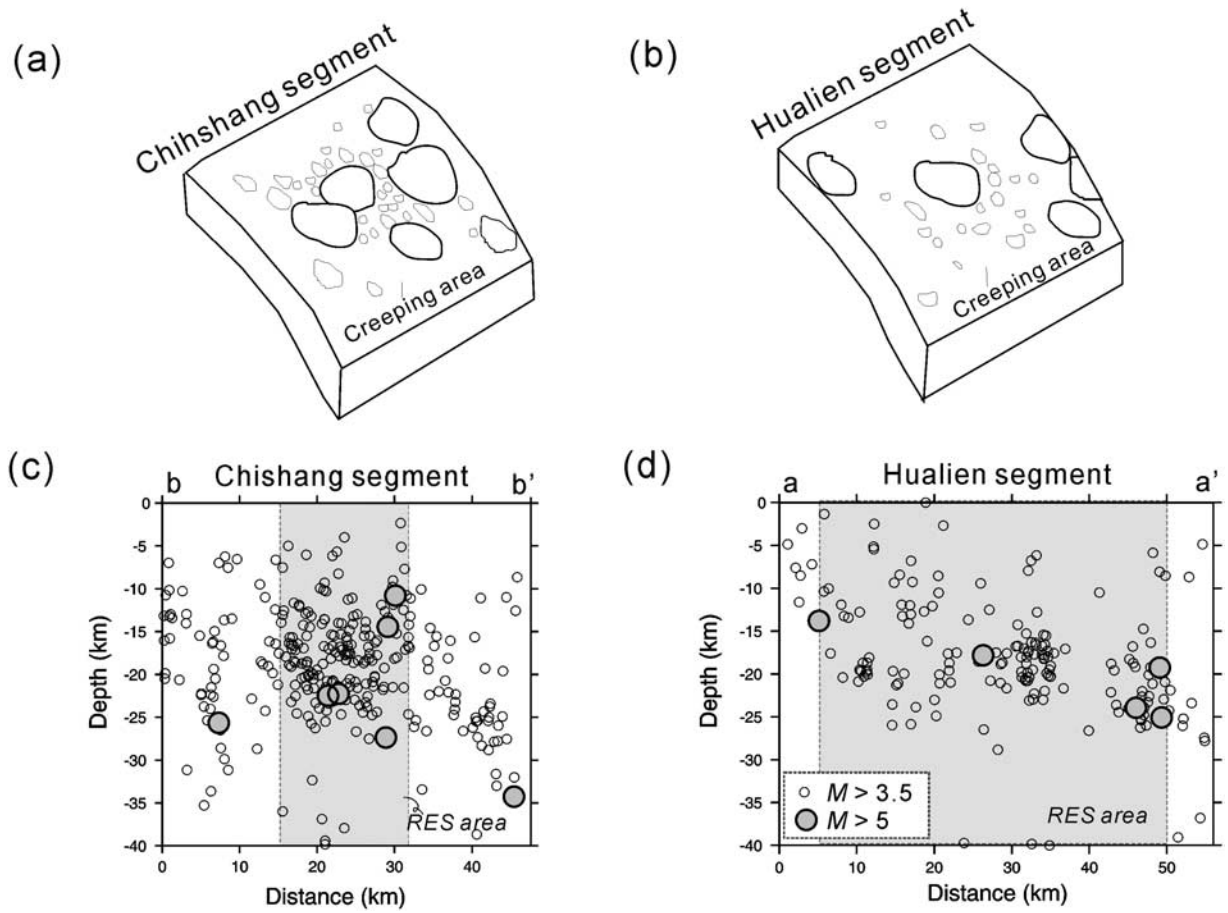

Figure 12. Schematic illustration of asperity distribution on the fault contact area for (a) the Chihshang segment and (b) the Hualien segment. Asperities of various sizes are surrounded by creeping areas. Larger open patches represent relatively large earthquakes ($M \sim 4$ or larger events in this study). Distance between the large events is shorter in the Chihshang segment, meaning that they are less isolated in space. Along-strike cross sections showing $M \geq 3.5$ earthquakes for (c) the Chihshang segment and (d) the Hualien segment. Profiles a-a′ and b-b′ with a width of 10 km are shown in Figure 1. The gray box indicates the area with RES observation.

action between two asperities is strong, which leads to complex recurrence behavior and possible change in the size and location of asperities. In this case the asperity may not occur in the same spot with similar size and may not have regular recurrence, so we cannot expect the repeated rupture of the asperity (i.e., repeating events). On the Hualien segment, the interaction between asperities is much weaker due to the longer separation distance between nearby large-sized asperities. These large earthquakes, therefore, are capable of rupturing repeatedly on this segment.

6.2.4. Summary and Other Factors

[36] The common features in fault loading rate and frequency-size distribution of background seismicity imply that the lack of $M \geq 3.8$ repeating events on the Chihshang segment is neither due to the relative lack of comparably sized earthquakes nor the slow loading rate of the fault. Statistical analysis on the size and number of earthquakes adjacent to RES indicates that the lower number of larger-sized earthquakes in the vicinity can explain the quasiperiodic recurrence of RES, and probably can explain the occurrence of RES of such size. We therefore infer a conceptual model that $M \sim 4$ or larger earthquakes should be isolated enough in space to facilitate the occurrence of repeated rupture. This plausible hypothesis will be tested as more repeating events data become available in the future with a sufficient range of magnitude.

[37] The sudden decrease of regional loading rates associated with large earthquakes, aseismic transient events, or slow slip events might contribute to the RES shutdowns of RES or unexpected changes in recurrence properties [*Nadeau et al.*, 1995; *Niu et al.*, 2003; *Nadeau and McEvilly*, 2004; *Templeton et al.*, 2008]. On the Chihshang segment, a M 6 large earthquake occurred at the end of the observation period. However, the associated postseismic effects on RES behavior have not yet been explored. Transient slip events can cause a sudden change in RES behavior [e.g., *Niu et al.*, 2003]. However, the first continuous GPS site in Taiwan was established in 1995, so knowledge about temporal changes of deep fault behavior induced by slow slip events is still limited.

[38] Rather than a mechanical explanation of the fault zone, it is still possible that some time-varying observational problems exist at the stations that were only used for RES identification near Chihshang, such as low detection capability, intermittent station outages, and temporally unstable noise characteristics of the records. These issues are not yet fully resolved. Better characterization of the fault zone properties and careful clarification of the observational issues will be essential for further investigation.

6.3. Are RES Characteristics Controlled by Specific Fault Properties?

[39] Repeating earthquakes that rupture the same fault patch are different from nonrepeating earthquakes in several ways. Repeating events are able to maintain their size and location over time, but nonrepeating earthquakes are not. In this case a mechanism that allows the fault patch to revert to its previous state over a certain range of area is required. A specific friction property that facilitates such healing has been referred to as stable creeping on the fault [*Anooshehpoor and Brune*, 2001; *Beeler et al.*, 2001; *Sammis and Rice*, 2001]. Localized deep aseismic slip, therefore, may be related to the frequent repeating earthquakes in the area. A fault zone characterized by higher clay mineral content, higher fluid content, and high pore pressure may initiate creep [e.g., *Sleep and Blanpied*, 1992; *Ben-Zion and Rice*, 1995].

[40] Strong stress heterogeneity on a fault is also a possible explanation for the occurrence of RES. *Marone et al.* [1995] reported an increase in stress drop over larger recurrence intervals from repeating earthquake data suggesting the asperity responsible for repeating events has high strength with a longer healing time. This kind of asperity is able to accumulate high stress. The unusually high stress drop for the small repeating events was later reported by *Nadeau and Johnson* [1998] using an empirical relationship between stress drop and magnitude of repeating events. The high stress drops of $\sim$100 MPa inferred from a kinematic source model for the sequence of M2 SAFOD target repeating earthquakes [*Dreger et al.*, 2007] supports this possibility. As discussed in Section 6.2.3 of this study, a specific asperity distribution is also relevant to the mechanism of repeating events. How lithological and geometric features affect RES characteristics, and whether there is a real limit to RES size on a fault are intriguing topics but are not yet understood. Further investigations on geological data, worldwide repeating earthquake data, and a well-resolved fault model are needed.

7. Conclusions

[41] We have investigated the similarities and variations in repeating earthquake behavior along fault segments in eastern Taiwan. Observations from 1991 to 2004 illustrate that between the Hualien and Chihshang segments, the characteristics of RES' regularity in size and timing vary little. While the Hualien segment produced events with a wide range of magnitudes of up to M 3.8 and M 4.6, the Chihshang segment only had RES of $M < 3.5$. The $M \geq 3.8$ RES on the Hualien segment is characterized by regular recurrence times and uniform rupture sizes. By calculating the number and size of the neighboring earthquakes around each RES we find that for the $M \geq 3.8$ RES, there are few surrounding earthquakes of large magnitude. The periodicity and size uniformity of these $M \geq 3.8$ RES, therefore, can be interpreted in terms of less influence from nearby earthquakes, where the degree of influence is controlled by the separation distance and relative size with respect to the RES. The absence of $M \geq 3.8$ RES on the Chihshang segment is unlikely to be explained by regional differences in fault loading rate and fault zone heterogeneity. We argue that the creeping area between $M \sim 4$ or larger earthquakes should be large enough to allow the spatial isolation of earthquakes of such size and therefore to facilitate the repeating ruptures over time. One implication of the variable size limit to RES magnitudes on faults is that the particular fault property facilitating creep may vary from one segment to the other.

[42] **Acknowledgments.** We thank Roland Bürgmann and Robert Nadeau for their helpful discussion and encouragement throughout this study and especially Leslie Hsu for her contributions in improving this manuscript. We are grateful to Associate Editor John Townend and two reviewers, Chung-Han Chan and Jian-Cheng Lee, for critical comments. This research was partially supported by Taiwan NSC grant 96-2116-M-006-011.

References

Abe, K. (1981), Magnitudes of large shallow earthquakes from 1904 to 1980, *Phys. Earth Planet. Inter.*, *27*, 72–92, doi:10.1016/0031-9201(81)90088-1.

Angelier, J., H. T. Chu, and J. C. Lee (1997), Shear concentration in a collision zone: Kinematics of the active Chihshang Fault, Longitudinal Valley, eastern Taiwan, *Tectonophysics*, *274*, 117–144, doi:10.1016/S0040-1951(96)00301-0.

Angelier, J., H. T. Chu, J. C. Lee, and J. C. Hu (2000), Active faulting and earthquake hazard: The case study of the Chihshang Fault, Taiwan, *J. Geodyn.*, *29*, 151–185, doi:10.1016/S0264-3707(99)00045-9.

Anooshehpoor, A., and J. N. Brune (2001), Quasi-static slip rate shielding by locked and creeping zones as an explanation for small repeating earthquakes at Parkfield, *Bull. Seismol. Soc. Am.*, *91*(2), 401–403, doi:10.1785/0120000105.

Ariyoshi, K., T. Matsuzawa, R. Hino, and A. Hasegawa (2007), Triggered non-similar slip events on repeating earthquake asperities: Results from 3D numerical simulations based on a friction law, *Geophys. Res. Lett.*, *34*, L02308, doi:10.1029/2006GL028323.

Astiz, L., and H. Kanamori (1984), An earthquake doublet in Ometepec, Guerrero, Mexico, *Phys. Earth Planet. Inter.*, *34*, 24–25, doi:10.1016/0031-9201(84)90082-7.

Barrier, E., J. Angelier, H. T. Chu, and L. S. Teng (1982), Tectonic analysis of compressional structure in an active collision zone: The deformation of the Pinanshan conglomerates, eastern Taiwan, *Proc. Geol. Soc. China*, *25*, 123–138.

Beeler, N. M., D. L. Lockner, and S. H. Hickman (2001), A simple stick-slip model for repeating earthquakes and its implication for microearthquakes at Parkfield, *Bull. Seismol. Soc. Am.*, *91*(6), 1797–1804, doi:10.1785/0120000096.

Ben-Zion, Y., and J. R. Rice (1993), Earthquake failure sequences along a cellular fault zone in a three-dimensional elastic solid containing asperity and nonasperity regions, *J. Geophys. Res.*, *98*, 14,109–14,131, doi:10.1029/93JB01096.

Ben-Zion, Y., and J. R. Rice (1995), Slip patterns and earthquake populations along different classes of faults in elastic solids, *J. Geophys. Res.*, *100*, 12,959–12,983, doi:10.1029/94JB03037.

Bürgmann, R., D. Schmidt, R. M. Nadeau, M. d'Alessio, E. Fielding, D. Manaker, T. V. McEvilly, and M. H. Murray (2000), Earthquake potential along the northern Hayward Fault, California, *Science*, *289*, 1178–1182, doi:10.1126/science.289.5482.1178.

Chen, H. H., and R. J. Rau (2003), Fault slip rates from repeating microearthquakes on the Chihshang fault, eastern Taiwan, *Eos Trans. AGU*, *84*(46), Fall Meet. Suppl., Abstract T11F-06.

Chen, H. K., R. Bürgmann, and R. M. Nadeau (2007a), Do repeating earthquakes talk to each other?, *Eos Trans. AGU*, *88*(52), Fall Meet. Suppl., Abstract S33C-1469.

Chen, K. H., R. M. Nadeau, and R. J. Rau (2007b), Towards a universal rule on the recurrence interval scaling of repeating earthquakes?, *Geophys. Res. Lett.*, *34*, L16308, doi:10.1029/2007GL030554.

Chen, K. H., R. M. Nadeau, and R. J. Rau (2008), Characteristic repeating microearthquakes on an arc-continent collision boundary—The Chihshang fault of eastern Taiwan, *Earth Planet. Sci. Lett.*, *276*, 262–272, doi:10.1016/j.epsl.2008.09.021.

Cheng, S. N., Y. T. Yeh, and M. D. Yu (1996), The 1951 Taitung earthquake in Taiwan, *J. Geol. Soc. China*, *39*(3), 267–285.

Ching, K. E., R. J. Rau, and Y. Zeng (2007), Coseismic source model of the 2003 Mw 6.8 Chengkung earthquake, Taiwan, determined from GPS measurements, *J. Geophys. Res.*, *112*, B06422, doi:10.1029/2006JB004439.

Dreger, D., R. M. Nadeau, and A. Morrish (2007), Repeating earthquake finite-source models: Strong asperities revealed on the San Andreas fault, *Geophys. Res. Lett.*, *34*, L23302, doi:10.1029/2007GL031353.

Ellsworth, W. L. (1995), Characteristic earthquakes and long-term earthquake forecasts, implications of central California seismicity, in *Urban Disaster Mitigation: The Role of Science and Technology*, edited by F. Y. Cheng and M. S. Sheu, pp. 1–14, Elsevier Sci., New York.

Gutenberg, R., and C. F. Richter (1954), *Seismicity of the Earth and Associated Phenomena*, 2nd ed., 310 pp., Princeton Univ. Press, Princeton, N. J.

Hsu, H. F. (1985), Analyzing the crustal movement and structure in eastern Taiwan from trilateration networks measurements (in Chinese), *Geod. Eng.*, *27*(1), 1–10.

Hsu, L., and R. Bürgmann (2006), Surface creep along the Longitudinal Valley fault, Taiwan from InSAR measurements, *Geophys. Res. Lett.*, *33*, L06312, doi:10.1029/2005GL024624.

Hu, J. C., J. Angelier, J. C. Lee, H. T. Chu, and D. Byrne (1996), Kinematics of convergence, deformation and stress distribution in the Taiwan collision area: 2-D finite-element numerical modeling, *Tectonophysics*, *255*, 243–268, doi:10.1016/0040-1951(95)00140-9.

Hu, J. C., et al. (2007), Coseismic deformation revealed by inversion of strong motion and GPS data: The 2003 Chengkung earthquake in eastern Taiwan, *Geophys. J. Int.*, *169*, 667–674, doi:10.1111/j.1365-246X.2007.03359.x.

Igarashi, T., T. Matsuzawa, and A. Hasegawa (2003), Repeating earthquakes and interplate aseismic slip in the northeastern Japan subduction zone, *J. Geophys. Res.*, *108*(B5), 2249, doi:10.1029/2002JB001920.

Johnson, K. M., P. Segall, and S. B. Yu (2005), A viscoelastic earthquake cycle model for Taiwan, *J. Geophys. Res.*, *110*, B10404, doi:10.1029/2004JB003516.

Johnson, P. A., and R. M. Nadeau (2002), Asperity model of an earthquake: Static problem, *Bull. Seismol. Soc. Am.*, *92*(2), 672–686, doi:10.1785/0120000282.

Kao, H., and P. R. Jian (2001), Seismogenic patterns in the Taiwan region: Insights from source parameter inversion of BATS data, *Tectonophysics*, *333*, 179–198, doi:10.1016/S0040-1951(00)00274-2.

Kao, H., S. J. Shen, and K. F. Ma (1998), Transition from oblique subduction to collision: Earthquakes in the southernmost Ryukyu arc-Taiwan region, *J. Geophys. Res.*, *103*, 7211–7229, doi:10.1029/97JB03510.

Kato, N. (2004), Interaction of slip on asperities: Numerical simulation of seismic cycles on a two-dimensional planar fault with nonuniform frictional property, *J. Geophys. Res.*, *109*, B12306, doi:10.1029/2004JB003001.

Kimura, H., K. Kasahara, T. Igarashi, and N. Hirata (2006), Repeating earthquake activities associated with the Philippine Sea plate subduction in the Kanto district, central Japan: A new plate configuration revealed by interplate aseismic slips, *Tectonophysics*, *417*, 101–118, doi:10.1016/j.tecto.2005.06.013.

Kuochen, H., Y. M. Wu, C. H. Chang, J. C. Hu, and W. S. Chen (2004), Relocation of eastern Taiwan earthquakes and tectonic implications, *Terr. Atmos. Oceanic Sci.*, *15*, 647–666.

Lay, T., and H. Kanamori (1980), Earthquake doublets in the Solomon Islands, *Phys. Earth Planet. Inter.*, *21*, 283–304, doi:10.1016/0031-9201(80)90134-X.

Lee, J. C., J. Angelier, H. T. Chu, J. C. Hu, F. S. Jeng, and R. J. Rau (2003), Active fault creep variations at Chihshang, Taiwan, revealed by creep meter monitoring, 1998–2001, *J. Geophys. Res.*, *108*(B11), 2528, doi:10.1029/2003JB002394.

Lee, W. H. K., F. T. Wu, and S. C. Wang (1978), A catalog of instrumentally determined earthquakes in China (magnitude 6 and larger) compiled from various sources, *Bull. Seismol. Soc. Am.*, *68*(2), 383–398.

Lynch, J. C., R. Bürgmann, M. A. Richards, and R. M. Ferencz (2003), When faults communicate: Viscoelastic coupling and earthquake clustering in a simple two-fault system, *Geophys. Res. Lett.*, *30*(6), 1270, doi:10.1029/2002GL016765.

Marone, C., J. E. Vidale, and W. L. Ellsworth (1995), Fault healing inferred from time-dependent variations in source properties of repeating earthquakes, *Geophys. Res. Lett.*, *22*, 3095–3098, doi:10.1029/95GL03076.

Massonnet, D., M. Rossi, C. Carmona, F. Adragna, G. Peltzer, K. Feigl, and T. Rabaute (1993), The displacement field of the Landers earthquake mapped by radar interferometry, *Nature*, *364*, 138–142, doi:10.1038/364138a0.

Matsubara, M., Y. Yagi, and K. Obara (2005), Plate boundary slip associated with the 2003 Off-Tokachi earthquake based on small repeating earthquake data, *Geophys. Res. Lett.*, *32*, L08316, doi:10.1029/2004GL022310.

Matsuzawa, T., T. Igarashi, and A. Hasegawa (2002), Characteristic small-earthquake sequence off Sanriku, northeastern Honshu, Japan, *Geophys. Res. Lett.*, *29*(11), 1543, doi:10.1029/2001GL014632.

Nadeau, R. M., and L. R. Johnson (1998), Seismological studies at Parkfield VI: Moment release rates and estimates of source parameters for small repeating earthquake, *Bull. Seismol. Soc. Am.*, *88*(3), 790–814.

Nadeau, R. M., and T. V. McEvilly (1999), Fault slip rates at depth from recurrence intervals of repeating microearthquakes, *Science*, *285*, 718–721, doi:10.1126/science.285.5428.718.

Nadeau, R. M., and T. V. McEvilly (2004), Periodic pulsing of characteristic microearthquakes on the San Andreas fault, *Science*, *303*, 220–222, doi:10.1126/science.1090353.

Nadeau, R. M., W. Foxall, and T. V. McEvilly (1995), Clustering and periodic recurrence of microearthquakes on the San Andreas fault at Parkfield, California, *Science*, *267*, 503–507, doi:10.1126/science.267.5197.503.

Niu, F., P. G. Silver, R. M. Nadeau, and T. V. McEvilly (2003), Migration of seismic scatters associated with the 1993 Parkfield aseismic transient event, *Nature*, *426*, 544–548, doi:10.1038/nature02151.

Peng, Z., and Y. Ben-Zion (2005), Spatio-temporal variations of crustal anisotropy from similar events in aftershocks of the 1999 M7.4 Ýzmit and M7.1 Duzce, Turkey, earthquake sequences, *Geophys. J. Int.*, *160*, 1027–1043, doi:10.1111/j.1365-246X.2005.02569.x.

Rau, R.-J., K. H. Chen, and K.-E. Ching (2007), Repeating earthquakes and seismic potential along the northern Longitudinal Valley fault of eastern Taiwan, *Geophys. Res. Lett.*, *34*, L24301, doi:10.1029/2007GL031622.

Ross, S. L., A. J. Michael, W. L. Ellsworth, B. Julian, F. Klein, D. Oppenheimer, and K. Richards-Dinger (2001), Effects of initial location error and station distribution on double-difference earthquake relocation: Comparing the San Gregorio and Calaveras faults, *Seismol. Res. Lett.*, *72*, 291–292.

Rubin, A. M. (2002), Using Repeating Earthquakes to correct high-precision earthquake catalogs for time-dependent station delays, *Bull. Seismol. Soc. Am.*, *92*(5), 1647–1659, doi:10.1785/0120010180.

Rubin, A. M., D. Gillard, and J. L. Got (1999), Streaks of microearthquakes along creeping faults, *Nature*, *400*, 635–641, doi:10.1038/23196.

Rubinstein, J. L., N. Uchida, and G. C. Beroza (2007), Seismic velocity reductions caused by the 2003 Tokachi-Oki earthquake, *J. Geophys. Res.*, *112*, B05315, doi:10.1029/2006JB004440.

Sammis, C. G., and J. R. Rice (2001), Repeating earthquakes as low-stress-drop events at a border between locked and creeping fault patches, *Bull. Seismol. Soc. Am.*, *91*(3), 532–537, doi:10.1785/0120000075.

Sammis, C. G., R. M. Nadeau, and L. R. Johnson (1999), How strong is an asperity?, *J. Geophys. Res.*, *104*, 10,609–10,619, doi:10.1029/1999JB900006.

Schaff, D. P., and G. C. Beroza (2004), Coseismic and postseismic velocity changes measured by repeating earthquakes, *J. Geophys. Res.*, *109*, B10302, doi:10.1029/2004JB003011.

Schaff, D. P., G. C. Beroza, and B. E. Shaw (1998), Postseismic response of repeating aftershocks, *Geophys. Res. Lett.*, *25*, 4549–4552, doi:10.1029/1998GL900192.

Scholz, C. H. (1990), *The Mechanics of Earthquakes and Faulting*, 439 pp., Cambridge Univ. Press, Cambridge, U. K.

Sleep, N. H., and M. L. Blanpied (1992), Creep, compaction and the weak rheology of major faults, *Nature*, *359*, 687–692, doi:10.1038/359687a0.

Templeton, D., R. M. Nadeau, and R. Bürgmann (2008), Behavior of repeating earthquake sequences in central California and the implications for subsurface fault creep, *Bull. Seismol. Soc. Am.*, *98*(1), 52–65, doi:10.1785/0120070026.

Turcotte, D. L. (1989), Fractals in geology and geophysics, *Pure Appl. Geophys.*, *131*, 171–196, doi:10.1007/BF00874486.

Uchida, N., T. Matsuzawa, T. Igarashi, and A. Hasegawa (2003), Interplate quasi-static slip off Sanriku, NE Japan, estimated from repeating earthquakes, *Geophys. Res. Lett.*, *30*(15), 1801, doi:10.1029/2003GL017452.

Vidale, J. E., W. L. Ellsworth, A. Cole, and C. Marone (1994), Variations in rupture process with recurrence interval in a repeated small earthquake, *Nature*, *368*, 624–626, doi:10.1038/368624a0.

Waldhauser, F., and W. L. Ellsworth (2000), A double-difference earthquake location algorithm: Method and application to the northern Hayward fault, California, *Bull. Seismol. Soc. Am.*, *90*(6), 1353–1368, doi:10.1785/0120000006.

Wang, W. H., and S. M. Huang (2006), Seismicity and stress evolution in heterogeneous faults with various degrees of roughness, *Tectonophysics*, *424*, 307–318, doi:10.1016/j.tecto.2006.03.042.

Working Group on California Earthquake Probabilities (2003), Earthquake probabilities in the San Francisco Bay region: 2002 to 2031, *U.S. Geol. Surv. Open File Rep.*, *03-214*.

Wu, F. T., R. J. Rau, and D. Salzberg (1997), Taiwan orogeny: Thin-skinned or lithospheric collision?, *Tectonophysics*, *274*, 191–220, doi:10.1016/S0040-1951(96)00304-6.

Yu, S. B., and L. C. Kuo (2001), Present-day crustal motion along the Longitudinal Valley Fault, eastern Taiwan, *Tectonophysics*, *333*, 199–217, doi:10.1016/S0040-1951(00)00275-4.

Yu, S. B., and C. C. Liu (1989), Fault creep on the central segment of the Longitudinal Valley fault, eastern Taiwan, *Proc. Geol. Soc. China*, *32*, 209–231.

Zöller, G., M. Holscheider, and Y. Ben-Zion (2005), The role of heterogeneities as a tuning parameters of earthquake dynamics, *Pure Appl. Geophys.*, *162*, 1027–1049, doi:10.1007/s00024-004-2660-9.

K. H. Chen, Department of Earth Sciences, National Taiwan Normal University, Number 88, Section 4, Tingzhou Road, Wenshan District, Taipei 116, Taiwan.

J.-C. Hu, Department of Geosciences, National Taiwan University, Number 1, Section 4 Roosevelt Road, Taipei 106, Taiwan.

R.-J. Rau, Department of Earth Sciences, National Cheng Kung University, 1 University Road, Tainan 701, Taiwan. (raurj@mail.ncku.edu.tw)